IR Investigation of the Oxidation of Propane and Likely C_3 and C_2 Products over Group IVB Metal Oxide Catalysts

M. A. Hasan,[†] M. I. Zaki,*[,‡] and L. Pasupulety[†]

Chemistry Department, Faculty of Science, Kuwait University, P.O. Box 5969, Safat, 13060 Kuwait, and Chemistry Department, Faculty of Science, Minia University, El-Minia 61519, Egypt

Received: June 18, 2002; In Final Form: October 4, 2002

In-situ infrared spectroscopy was used to examine the gas phase and adsorbed species formed during the oxidation of propane gas on ZrO_2, TiO_2, and CeO_2 catalysts, versus a reference Pt/Al_2O_3 catalyst, in the absence and presence of an oxygen atmosphere. The same examination was applied to a number of likely oxidation products, namely, 2-propanol, acetone, and acetic acid (vapor phase). Both examinations were carried out as a function of temperature (up to 400 °C). The results obtained could help in assigning the oxidation pathway and surface sites, which are considered extendable to metal oxide surfaces containing no excess oxygen species. A number of important conclusions were, accordingly, arrived at, the most prominent of them being: (i) the initial catalytic interaction is the oxidative dehydrogenation of propane into propene, rather than the oxidative addition into 2-propanol; (ii) the catalytic activity of the test oxides (ZrO_2 < TiO_2 < CeO_2) appears to be directly related to the oxide reducibility and surface acidity; (iii) the catalytic active sites are Lewis acid−base pair sites over which the secondary carbon C−H bond is activated by simultaneous bonding, and the hydrogen abstraction is facilitated by the reducibility of the Lewis acid site; (iv) CeO_2 is a promising catalytic material for the total oxidation of hydrocarbons.

Introduction

Natural gas-fueled turbines are promising thrusters for electric power generators.[1] The propellant gas is produced via total oxidation (combustion) of the natural gas (essentially methane) in sufficient oxygen atmosphere. Conventionally, the combustion process is flame-activated.[1] The exothermic nature of the process, together with the thermal energy supplied by the flame, results in the buildup of high-temperature regimes (1300−1500 °C) and, hence, high emission levels of NO_x in the exhaust.[1,2] Therefore, a catalytic combustion process is sought worldwide to reduce the combustion temperature (<1300 °C) and the environmental risk of the NO_x emissions.

Metal-oxide-based catalysts are increasingly tested as replacements for the active, but unstable, noble metal (e.g., Pt and Pd) combustion catalysts, although with limited success. Noble metals are susceptible to sintering and form volatile oxides under the combustion conditions.[1] Hitherto, however, a few metal oxide composites, mostly assuming perovskite[1−4] and spinel[5] structures, or dispersed on thermally stable ceramic supports (viz., cordierite, mullite, and aluminum titanate),[1,6,7] have been considered promising. The oxidation activity of these metal oxides has been found[2−4] to optimize in an electron-mobile environment established by d−d electron exchange interactions involving metal atoms of different oxidation states.

Despite their limited success in combustion (total oxidation) reactions of hydrocarbons, metal oxide catalysts are quite successful in partial oxidation reactions of olefins,[8] light alkanes,[9] and aromatics.[10] This fact may be considered incompatible with the results of a relatively more recent IR study[11] of catalytic oxidation of C_1−C_4 hydrocarbons on $MgCr_2O_4$, which shows total oxidation of the test hydrocarbons to be consecutive to their partial oxidation. The study[11] suggests, moreover, that: (i) C−H bonds are the active moieties in oxidizable hydrocarbons; (ii) the C−H activity is inversely related to the bond dissociation energy, but directly related to the bonding symmetry of the carbon atom (tertiary > secondary > primary carbons); (iii) the total oxidation to CO_2 and H_2O is intermediated by formation (and subsequent oxidation) of several oxygenate compounds (alkoxidic, aldehydic, ketonic, and/or carboxylic species); (iv) on metal oxides exposing strong base sites, the initial catalytic step involves electronic interactions between nonbonding orbitals of surface oxide (O^{2-}) sites and antibonding (σ^*) orbitals of the C−H bond, whereas it involves the interaction between d-type orbitals of the surface metal (M^{n+}) sites and both σ and σ^* orbitals of the C−H bond on oxides exposing strong acid sites; and (v) active surface oxygen species could equally be nucleophilic (O^{2-}) or electrophilic ($O^{<2-}$). It is worth noting that suggesting the involvement of nucleophilic O^{2-} surface species in total oxidation reactions contradicts long standing findings by Haber,[9,12] whereas suggesting Lewis acid sites (M^{n+}) to initiate the activation of C−H bonds is in line with earlier results of Al-Mashta et al.[13] as well as recent results of Zaki et al.[14] The formation of π-complexes of olefins with cations, like Pt^{2+}, Fe^{3+}, Cu^{2+}, or Cr^{3+},[15] or even d^0 cations, like Ti^{4+} or Zr^{4+},[16] both on the surface and in homogeneous complexes, is also supportive to the latter suggestion.

In line with the current research endeavors toward the design of active and durable metal oxide combustion catalysts, the present in-situ IR study of catalytic combustion of propane, 2-propanol (2-propanol), acetone, and acetic acid in rich O_2 atmosphere (at up to 400 °C) on Group IVB metal oxides (TiO_2, ZrO_2, and CeO_2) was undertaken. Equilibrium reaction products were identified both on the surface and in the gas phase. The

* Corresponding author. Tel & Fax: 02-086-360833. E-mail: mizaki@link.net.
[†] Kuwait University.
[‡] Minia University.

10.1021/jp0214413 CCC: $22.00
Published on Web 11/14/2002

test catalysts were chosen on the following basis: (i) their surfaces have various acid−base properties and sites,[17,18] (ii) the metal sites thereon exposed assume disparate reducibilities, (iii) their oxidative dehydrogenation activities are disparate,[19,20] and (iv) the fact that they have, hitherto, not been tested in such IR studies of catalytic combustion. To assess and rank the combustive activity of the test catalysts, a Pt/Al_2O_3 catalyst was prepared and used in the combustion of propane. The principal objective of the present investigation was to facilitate a better understanding of (i) the interrelations between the total and partial oxidation pathways, (ii) the C−H activation step on metal oxide surfaces, and (iii) the nature of the oxidant oxygen species.

Experimental Section

Test Metal Oxide Catalysts. The metal oxide catalysts were ∼99% pure P25 titania (anatase TiO_2, 50 m^2/g), MEL zirconia ((monoclinic + tetragonal) ZrO_2, 34 m^2/g), and Rhône-Polenc ceria (fluorite CeO_2, 31 m^2/g). They were used as supplied.

Reference Pt/Al_2O_3 Catalyst. The Pt/Al_2O_3 catalyst was synthesized by in-situ heating of H_2PtCl_6-impregnated Al_2O_3 in a stream of H_2 (inside the IR-cell, vide infra) at 200 °C for 2 h. The Pt precursor compound was a 99.9% pure Fluka product, the alumina a Degussa aluminum oxide C ($(\gamma+\delta)$-Al_2O_3, 107 m^2/g), and the impregnation was done in aqueous medium (at room temperature, RT). The impregnation was followed by evaporation of the excess water at 80 °C, drying at 100 °C for 48 h, and resulted in a 7 wt %-Pt in the final catalyst as determined by atomic absorption spectrometry.

Reactants and Gases. Reactant molecules were provided by expanded vapors of 2-propanol (denoted IPr), acetone (Ac), and acetic acid (AcAc) at RT—their source liquids being AR-grade products of BDH. They were deaerated prior to application, by on-line freeze−pump−thaw cycles performed at liquid nitrogen temperature (−195 °C). Propane, O_2, and H_2 gases were 99.99% pure products of KOAC (Kuwait) and were used as supplied. Propane was the hydrocarbon reactant, O_2 was used to burn off surface impurities in the in-situ pretreatment of the oxide wafers, and H_2 was the reductant used to synthesize the Pt/Al_2O_3 catalyst.

In-situ IR Spectroscopy. FTIR spectra were taken of the gas phase and adsorbed species, using a specially designed[21] all-Pyrex glass IR-cell equipped with CaF_2 windows and hooked to a homemade gas/vacuum handling system, and a model Spectrum-BX FTIR Perkin-Elmer spectrometer. Self-supporting, thin wafers (∼20 mg/cm^2) of test catalysts were mounted inside the cell. They were briefly outgassed at RT, heated in a stream of O_2 (50 cm^3/min) at 400 °C for 1 h, outgassed at 300 °C for 1 h, and cooled under vacuum to RT, prior to exposure to the reactant molecules. Only in the case of Pt/Al_2O_3, the preliminary evacuation at RT was followed by heating in a stream of H_2 (50 cm^3/min) at 400 °C (for 2 h), prior to a final outgassing at the same temperature for 1 h and cooling to RT. The reactant atmosphere (10−3 Torr, depending on the vapor pressure of the liquid reactants at RT) was maintained in contact with the catalyst wafer (at the temperature applied) for 10 min. Then, the temperature was leveled off to RT. Following the recording of spectra of the gas phase, the gas phase was pumped off for 5 min, and spectra were taken of the "catalyst + adsorbed species". By absorption subtraction of the catalyst background spectrum, a difference spectrum of the "adsorbed species" was obtained.

Results and Discussion

Stability of Reactants versus Pyrolysis and Molecular Oxygen. Figure 1 shows that the IR spectra taken of the propane gas phase following heating in the absence of oxygen atmosphere (i.e., gas-phase molecules) at 100, 200, 300, and 400 °C were identical to the spectrum taken at RT. In the presence of oxygen, however, though spectra taken at ≤200 °C were one-and-the-same, those observed at 300 and 400 °C showed some minor, but significant, differences. It is revealed, in Figure 1, that these differences are due to the emergence of weak (to very weak) bands at 2344, 2140, 1743, 1649, 1425, 1366, 1272, and 1150 cm^{-1}, as well as a set of weak, but sharp, bands at 1030, 988, 946, and 913 cm^{-1}. As assigned in Figure 1, the former two bands are indicative of the formation of CO_2 and CO molecules,[22] whereas the latter set of four bands (1030−913 cm^{-1}) indicate formation of propene (C_3H_6) molecules.[23] On the other hand, the six bands at 1743−1150 cm^{-1} are very close to those reported[24] for acrolein (CH_2═$CH-CHO$). A quantitative processing of the spectra, using P-E Spectrum version 2.0 software, revealed that the overall conversion of the propane gas (10 Torr) at 400 °C in the presence of oxygen does not exceed 3%.

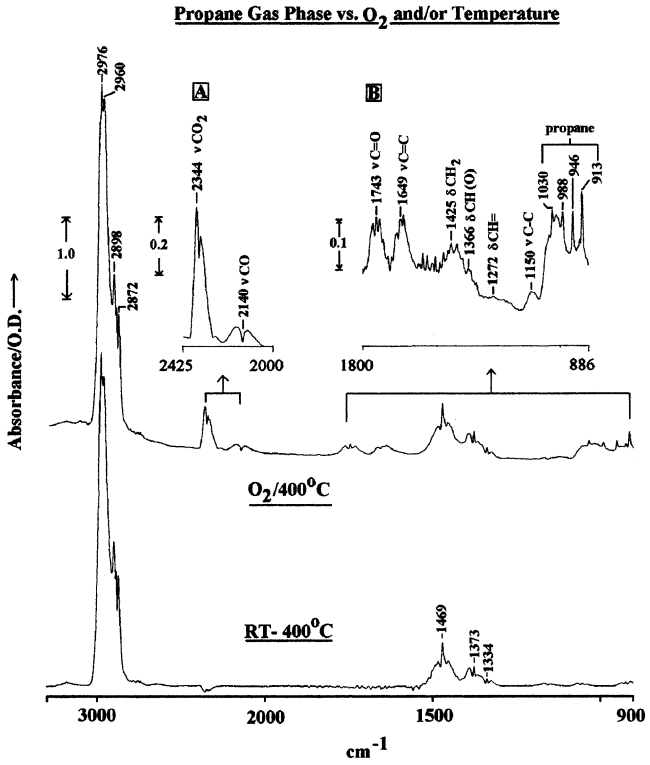

Figure 1. FTIR spectra taken of 10-Torr propane gas phase at RT, and following heating at various temperatures (100−400 °C) for 10 min, in the absence and presence of 50-Torr oxygen atmosphere. The insets [A] and [B] are expansions of the corresponding portions of the spectra taken at 400 °C in the presence of oxygen.

Figure 2 displays the results of similar stability tests for the gas phase of the oxygenate compounds IPr (2-propanol), Ac (acetone), and AcAc (acetic acid). It is obvious from the spectra therein exhibited that the three oxygenate compounds are stable to heating to 400 °C in the absence of oxygen. In the presence of oxygen, however, these molecules could not withstand heating to ≥300 °C. The spectra obtained following heating at 400 °C in an oxygen atmosphere (Figure 2) indicate 89%con (overall conversion) of IPr into CO_2 and acetone molecules, 34%con of Ac into CO_2, and 87%con of AcAc into CO_2.

The above results can lead to the following facts. All of the reactants (propane and oxygenates) are stable to pyrolysis on heating to 400 °C. In the presence of oxygen, ca. 3% of the amount of propane is oxidized at 400 °C, giving rise to total

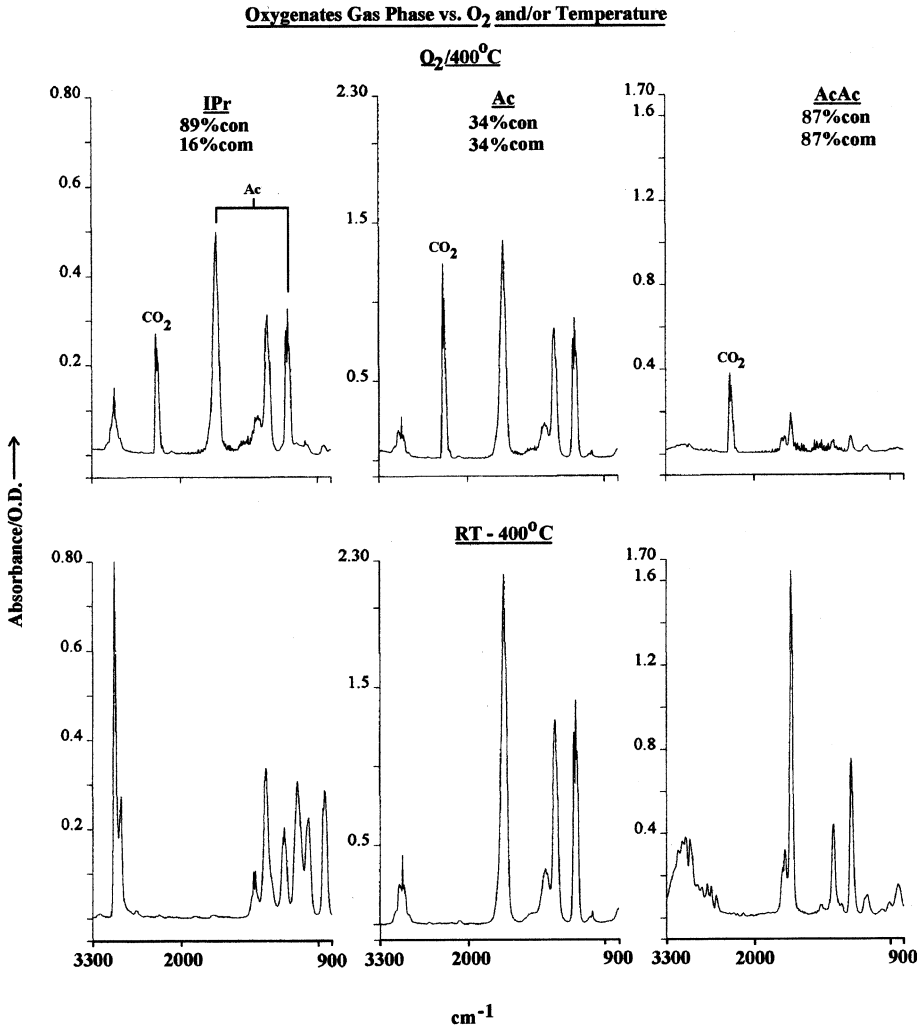

Figure 2. FTIR spectra taken of the gas phase of 10-Torr 2-propanol (IPr), 10-Torr acetone (Ac), and 3-Torr acetic acid (AcAc) at RT, and following heating at various temperatures (100−400 °C) for 10 min, in the absence and presence of five times the oxygenate pressure of oxygen atmosphere [%con = %conversion; %com = %combustion].

(CO_2) and partial (acrolein) oxidation products, as well as an oxidative dehydrogenation product (propene).[24] In contrast, overoxidation of the oxygenate compounds (combustion = com) is triggered only at 400 °C. IPr and AcAc show a much higher oxidizability (87−89%con) than Ac (34%con). However, AcAc and Ac are similarly totally oxidized to CO_2, whereas IPr is mostly (73%) partially oxidized to acetone with a minor (16%com) total oxidation to CO_2. It is worth noting that water, the other total oxidation product, manifested itself in the spectra by a broad band at 3300−3200 cm^{-1} due to hydrogen bonding. According to Finocchio et al.,[25] these facts may reveal that (i) the total oxidation may follow a partial oxidation of propane (→ alcohol → ketone → etc.) or of its oxidative dehydrogenation product (→ propene → acrolein → etc.); (ii) the much higher oxidizability of IPr, Ac, and AcAc than propane may explain their absence among the oxidation gas-phase products of the latter; and (iii) in the presence of oxygen molecules in the gas, a catalytic (surface) oxidation of propane cannot be discussed without consideration of a possible intervention of a noncatalytic (gas-phase) oxidation, particularly, of its partial oxidation products.

Catalytic Oxidation Activity and Gas-Phase Products. In absence of oxygen atmosphere, heating to 400 °C of propane gas phase over the three test oxide catalysts (ZrO_2, TiO_2, and CeO_2) resulted in hardly any detectable change to the chemical composition of the gas phase, except for the appearance of a very small amount of CO_2 molecules over CeO_2 at 400 °C only. CeO_2 is known for its much higher lattice oxygen (O^{2-}) mobility[26] than both TiO_2 and ZrO_2. In presence of oxygen atmosphere, IR examination of the influence of heating on propane monitored only insignificant oxidation at 300 °C over ZrO_2 and TiO_2, but a detectable oxidation over CeO_2. Increasing the temperature to 400 °C was found to improve the propane oxidation over all the test catalysts; however, the improvement remained proportional (i.e., more on CeO_2 than on both TiO_2 and ZrO_2). In Figure 3, the results obtained at 400 °C over the oxide catalysts are compared to those obtained in the absence of a catalyst or in the presence of the reference Pt/Al_2O_3 catalyst. It is obvious from the spectra displayed, as well as from results of their quantitative processing and νOH spectra obtained at 3300−3200 cm^{-1} (not shown), that the sole detectable gas-phase oxidation products over the oxide and metal catalysts are CO_2 and H_2O. This indicates that the catalysts enhance the overoxidation of the partial oxidation products observed in their absence (i.e., propene and acrolein, Figures 1 and 3). The total-oxidation activities of both ZrO_2 and TiO_2, as approximated by the %com (%combustion) accomplished on them (4 and 7%, respectively), are modest as compared to the activity of CeO_2 (42%com). The activity of the latter is almost half that of Pt/Al_2O_3 (92%), which is a standard combustion catalyst.[1] It is worth noting that the noncatalytic combustion involved, if any, does not exceed 1% (Figure 3).

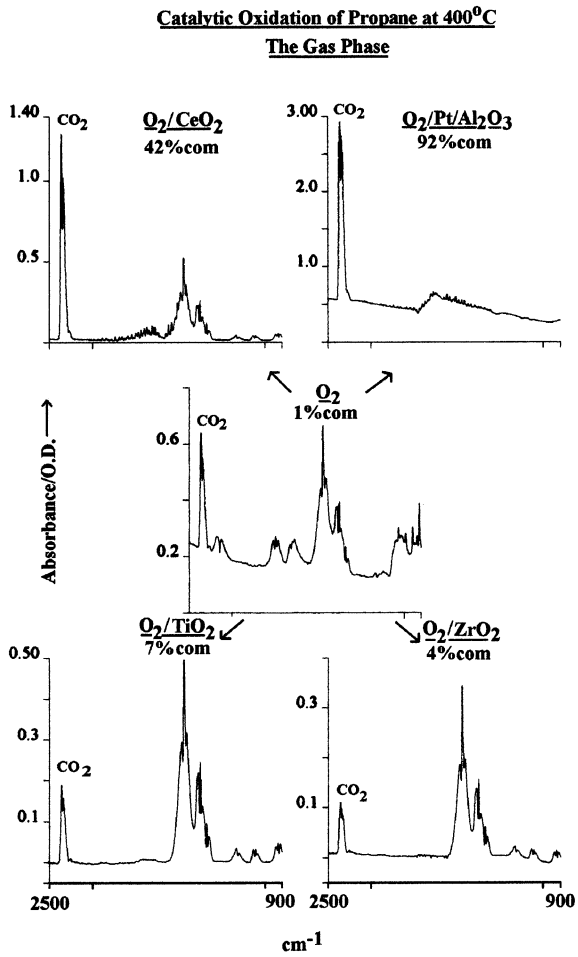

Figure 3. FTIR spectra taken of the gas phase of 10-Torr propane following heating at 400 °C for 10 min in oxygen atmosphere (50 Torr), in the presence and absence of the catalysts indicated.

To discover reasons behind the absence in the gas phase of propane oxidation products other than CO_2 and H_2O, the effect of temperature on the gas phase of IPr, Ac, and AcAc was IR-followed over the oxide catalysts in the presence of oxygen atmosphere. According to Finocchio et al.,[25] these three oxygenate compounds are conceivable partial oxidation products of propane in lean oxygen atmosphere. The results obtained showed the oxygenate compounds to withstand heating to 200 °C without oxidation. At 300 °C, however, they suffered various, but limited, extents of combustibility as per the following descending order: IPr > AcAc ≫ Ac. The detectable oxidation products of IPr were acetone, CO_2, and H_2O, the former being (a partial oxidation product) the major product on both ZrO_2 and TiO_2, while the latter two total oxidation products were the major products on CeO_2. In the case of Ac and AcAc, the sole detectable products were CO_2 and H_2O. Upon increasing the reaction temperature to 400 °C, the gas-phase spectra obtained (Figure 4) reveal an obvious development of the oxidation activity of the three test catalysts toward each of the oxygenate compounds, however, in the following order of combustibility: AcAc (78%) > IPr (76%) > Ac (70%). The %combustion parenthesized is an average value over the three catalysts, viz., for AcAc = [63%(ZrO_2) + 78%(TiO_2) + 93%-(CeO_2)]/3 = 78%. The results shown in Figure 4 can help in ranking the total oxidation activity of the test catalysts as follows: CeO_2 > TiO_2 ≫ ZrO_2. It is quite obvious from the spectra displayed in Figure 4 that the modest total oxidation activity of ZrO_2 is due to its inability to enhance the overoxidation of acetone.

The above results show that in the presence of oxygen molecules in the gas phase, the oxidative dehydrogenation of 2-propanol to acetone is much faster than the overoxidation of the product to eventually give CO_2 and H_2O, particularly on ZrO_2. On CeO_2, and to a lesser extent on TiO_2, the total oxidation course is very much enhanced. These experimental facts may help presuming the following: (i) if the initial oxidation step of propane were to result in the formation of 2-propanol and/or acetone, acetone molecules would have been detected in the gas phase at 300 °C, or even at 400 °C on ZrO_2, and (ii) the relative order of oxidation activity of the catalysts (CeO_2 > TiO_2 ≫ ZrO_2) parallels the order of their reducibilities,[27] thus suggesting an important role for the lattice oxygen in the oxidation course with a Mars-Van-Krevelen-type mechanism.[28]

In the search for a consolidation of the above presumptions, IR spectra were taken of surface species established during the oxidation course on the test catalysts, in the presence and absence of gas-phase oxygen . It is worth mentioning, however, that the signal/noise ratio of the spectra taken of the adsorbed species on CeO_2 was, unfortunately, much less than that of the spectra taken on the other two oxides. The main reason is that much thicker wafers (150−120 mg/cm^2) had to be prepared from CeO_2, to overcome the intolerance of its particles to compression into thin wafers of sufficiently high IR-transmission. Therefore, the presentation and discussion set out in the following sections are confined to the spectra taken of the adsorbed species on TiO_2 and ZrO_2. In fact, the sole spectrum presented for CeO_2, viz., the surface-OH spectrum (Figure 5), is obviously of lower quality than the spectra presented for the other two oxides (Figure 5).

Catalytic Oxidation Surface Species. IR spectra taken of the catalysts following the in situ pretreatment, and prior to exposure to the reactant atmospheres, monitored nothing but very weak absorptions at 1500−1300 cm^{-1} due to carbonaceous impurity species, weak νCH absorptions at 2950−2850 cm^{-1} originating from hydrocarbon impurity species, and the νOH absorptions displayed in Figure 5. According to earlier reports, the high-frequency νOH band (3772 cm^{-1}) of ZrO_2 is indicative of terminal Zr−OH groups,[29] whereas the low-frequency one (3674 cm^{-1}) conceals another band at 3668 cm^{-1}. The latter two bands are due to two different multicentered $(Zr)_xOH$ groups.[29] The weak band at 3734 cm^{-1} is due to Si−OH groups originating from silica impurity species in ZrO_2, as admitted by the manufacturer.[17] The νOH-spectrum presented for TiO_2 (Figure 5) is similar to that obtained previously,[17] and, thus, the three bands therein monitored can, accordingly,[17] be assigned to two different types of terminal Ti−OH groups (3718 and 3665 cm^{-1}) and a bridging $(Ti)_2OH$ group (3642 cm^{-1}). According to Tsyganenko and Filimonov,[30] fluorite-structured CeO_2 should expose various types of OH-groups: terminal (3690−3680 cm^{-1}), bridging (3650−3640 cm^{-1}), multicentered (3630−3610 cm^{-1}), and hydrogen-bonded (<3600 cm^{-1}) OH groups. Hence, the ill-defined bands observed in the νOH-spectrum of CeO_2 (Figure 5) may be ascribed to the exposure of terminal Ce−OH (3689 cm^{-1}), bridging $(Ce)_2OH$ (3644 cm^{-1}), and hydrogen-bonded OH groups (3517 cm^{-1}). However, the possibility still stands for the coexistence of multicentered $(Ce)_xOH$ groups (ca. 3600 cm^{-1}). In terms of the inverse relationship existing between the magnitude of the νOH-frequency and the OH-acidity,[17,31] the relatively most acidic OH

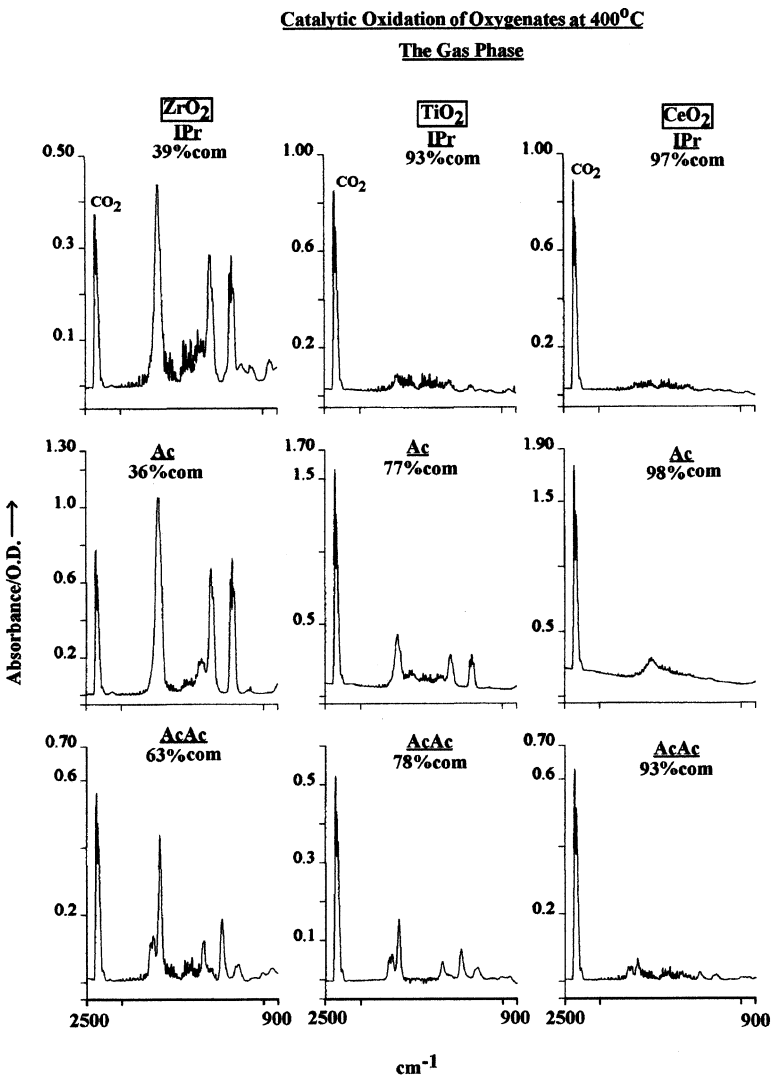

Figure 4. FTIR spectra taken of the gas phase of isoropanol (IPr, 10 Torr), acetone (Ac, 10 Torr), and acetic acid (AcAc, 3 Torr), following heating at 400 °C for 10 min in the presence of oxygen atmosphere (5 times the oxygenate pressure) and the catalysts indicated.

groups should be those exposed on CeO_2, whereas the most basic ones should be those found on ZrO_2.

Figure 6 displays spectra which were taken of the surface species established on TiO_2 (and ZrO_2; the insets (a) and (b)) upon heating the interfaces with propane at 200° and 400 °C, in the absence and presence of oxygen atmosphere. It is worth noting that the spectra obtained at RT and 100 °C showed insignificant surface interactions, whereas those obtained at 300 °C were similar to the 400 °C spectra. In the absence of oxygen, the 200 °C spectra reveal that the surface interactions resulted in the elimination (or association) of the oxide surface-OH's (Figure 5) as indicated by the negative absorptions at corresponding frequencies (Figure 6). Instead, the spectra monitor the emergence of νOH-bands at the higher frequencies of 3620, 3465, and 3410 cm^{-1}. The spectra also monitor νCH-bands at 2953, 2922, and 2852 cm^{-1}, a strong νC═O/νC═C-band at 1617 cm^{-1}, and weak $\nu COO^-/\delta$CH/νC−C-bands at 1524−1126 cm^{-1}. In the presence of oxygen, the significant modifications observed in the 200 °C spectra are (i) elimination of the νOH-band at 3620 cm^{-1}, as well as the three νCH-bands at 2953−2852 cm^{-1}; (ii) a general reinforcement of the $\nu COO^-/\delta$CH-bands at 1540−1257 cm^{-1}; and (iii) generation of strong bands at 1416 and 1345 cm^{-1}. Upon increasing the temperature to 400 °C, whether in the presence or absence of oxygen atmosphere, the spectra obtained (Figure 6) are similar in displaying three strong bands at 1621−1617, 1551−1547, and 1435−1431 cm^{-1}, and three weak, but sharp, bands at 1471−1470, 1377, and 1355−1350 cm^{-1}. On ZrO_2, no detectable absorption is observed at 1621−1617 cm^{-1}. To properly assign these bands to the relevant surface species of propane and its oxidation products, IR spectra were also taken of adsorbed species of the oxygenate compounds (IPr, Ac, and AcAc) as a function of temperature. Some of the spectra obtained are presented and discussed below.

Figure 7 presents the spectra obtained (at 1800−1000 cm^{-1}) for the adsorption of IPr, Ac, and AcAc on TiO_2 at RT, 200°, and 400 °C in the presence of oxygen atmosphere. The corresponding νCH-spectra (at 3000−2800 cm^{-1}) are also presented in insets (a), (b) and (c), respectively, of Figure 7. It is worth mentioning, that a largely similar set of spectra were obtained for the adsorption of each oxygenate compound on ZrO_2. For IPr, the RT-spectra (Figure 7A) monitor bands that have been frequently observed and reported[19,20] for νCH (2961−2844 cm^{-1}), δCH (1462−1335 cm^{-1}), νC−C (1169 and 1130 cm^{-1}), and νC−O (1014 cm^{-1}) of isopropoxide species. The weak band at 1265 cm^{-1} is rather close to the δOH-band of alcohol molecules bound to the surface via the oxygen atom.[19,20] The splitting of the νC−C band to occur at 1169 and 1130 cm^{-1} has been attributed[31] to the occurrence of the isopropoxide species in two different bonding configurations, namely terminal

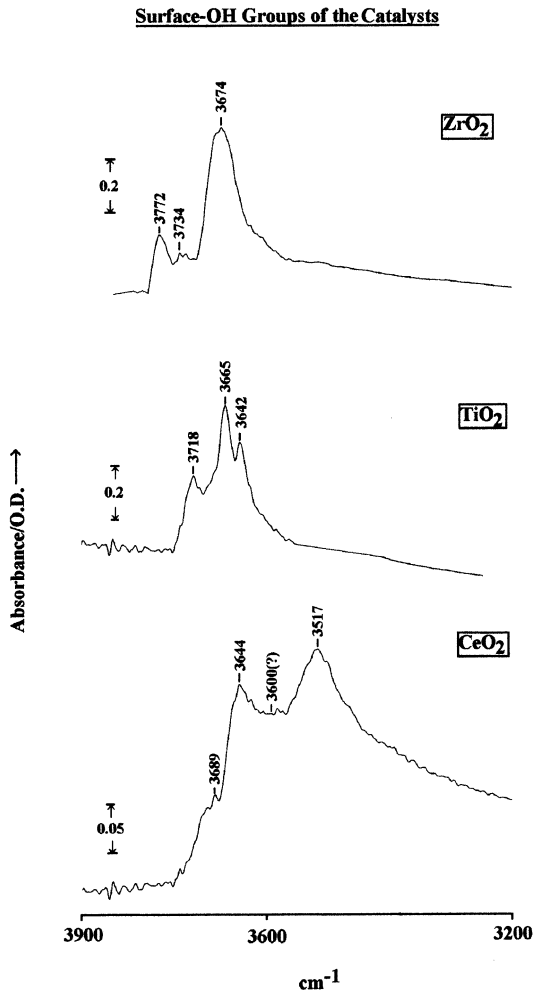

Figure 5. FTIR νOH-spectra taken at RT of the catalysts indicated, following the in-situ pretreatment, and prior to the exposure to the reactant atmosphere.

and bridging species. At 200 °C, the spectrum obtained monitors weakening of the isopropoxide features, and the emergence of two weak bands at 1567 and 1428 cm^{-1}. At 400 °C, these two bands are developed into two very strong absorptions, now at 1547 and 1455 cm^{-1}, together with the other weaker features displayed (at 1693, 1342, 1049, and 1022 cm^{-1}, Figure 7A). These two bands, being assignable, respectively, to the $\nu_{as}COO^-$ and ν_sCOO^- vibrations, suggest transformation of the isopropoxide species into acetate species.

Acetone (Ac) adsorption at RT resulted in spectra (Figure 7B) revealing the conversion of the adsorptive molecules into conjugated carbonyl species giving rise to low-frequency νC═O (1694 cm^{-1}) and νC═C (1594 cm^{-1}), as well as a number of weak absorptions due to δCH (1459−1219 cm^{-1}) and νC−C/νC−O (1169−1033 cm^{-1}), assignable to aldol-condensation products (diacetone alcohol and/or mesityl oxide).[34,35] Thus, acetone molecules are activated on the surface for aldol-condensation type of interaction at RT. At ≥200 °C, the spectra obtained (Figure 7B) display bands similar to those shown by IPr/TiO_2 at 400 °C (Figure 7A), i.e., due to acetate surface species. The shoulder at 1617 cm^{-1} may possibly be due to νC═C vibrations of acrylate-like species.[25,36] These results indicate that the condensation products of acetone are readily oxidized on the surface as of a temperature as low as 200 °C. That the eventual surface oxidation products of IPr and Ac are acetate species can be evidenced by the spectral features of the adsorbed species of acetic acid (AcAc) as a function of temperature (Figure 7C). The acetate species established at RT are stable to heating to 400 °C, giving rise to the diagnostic antisymmetric and symmetric stretching vibrations of their caboxylate groups at 1544 and 1462 cm^{-1}, respectively.

The above results can exclude attributing the IR absorptions observed for propane/TiO_2 at 200 °C in absence of O_2 atmosphere (Figure 6A) to isopropoxide or acetone condensation products. They may, instead, assign them to acrylate-like species, adopting the acrylate characteristic absorptions reported by Finocchio et al.:[25] 1640 (νC═C), 1500 ($\nu_{as}COO^-$), 1440 (ν_sCOO^-), and 1370 and 1270 cm^{-1} (δCH). The fact that the νC═C vibration is observed here at a lesser frequency (1621−1617 cm^{-1}) may be due to the fact that the present surfaces were not as oxidized as their test surfaces (chromate-covered $MgCr_2O_4$ surfaces). Hence, the double bond π-electrons are more involved in surface bondings on the present catalysts. The suggested acrylate-like species are further oxidized to acetate (and possibly formate) species at 400 °C in the presence of oxygen atmosphere. A co-formation of carbonaceous species, carbonate/bicarbonate, may have some support from the presence of the low-frequency νOH vibrations (namely, the 3410 cm^{-1} band) as well as the 1355−1350 cm^{-1} band. It is noteworthy that, unlike the case on TiO_2, the spectra taken from propane/ZrO_2 at 400 °C (Figure 6, the insets (b)) are void of any significant absorption but the bands characteristic of surface acetate species. Thus, whether the 1621−1617 cm^{-1} band is due to νC═C vibrations of the acrylate species or $\nu_{as}COO^-$ of the bicarbonate species, neither of these species form or stabilize on ZrO_2 surfaces. This may mean that the formation (or stabilization) of the species responsible for this band (1621−1617 cm^{-1}) requires a highly mobile surface oxygen, which is more available on TiO_2 than ZrO_2 (the former is more reducible than the latter).[27]

Adsorptive and Catalytic Events in the Oxidation Course. The oxidation of propane in the presence of oxygen molecules in the gas phase and a metal oxide catalyst (MO_2) might involve different oxidant species: (i) oxygen radicals (O) produced by homolytic fission of molecular oxygen bonds at ≥300 °C, and (ii) surface oxygen species, either lattice oxygen (O^{2-}) or adsorbed oxygen (O_2^{x-}, O^-, or O^{2-}). Therefore, we will denote the process involving oxygen radicals by "gas-phase oxidation", whereas that involving surface oxygen by "surface oxidation". The oxidation pathways observed are also different: (i) oxidative dehydrogenation, (ii) partial (selective) oxidation, and (iii) total (combustive) oxidation. Whereas products of partial oxidation of propane are often C_3 (2-propanol and acetone), C_2 (acetic acid), and C_1 (formic acid) oxygenate compounds,[25] total oxidation products are only CO_2 and H_2O. On the other hand, oxidative dehydrogenation products include propene, as well as propene C_3−C_1 oxidation products (e.g., allyl alcohol, acrolein, acrylic acid, acetic acid, etc.).[25]

The results shown in Figures 1 and 2 are indicative of the occurrence of gas-phase oxidation of propane, IPr, Ac, and AcAc, on the basis of their evident thermal stability (in the absence of oxygen). The gas-phase oxidation of propane (at 400 °C) is insignificant (3%con, 1%com) as compared to that of AcAc (87%con,com), Ac (34%con,com), and IPr (89%con, 16%com). The evident thermal stability of the substrate molecules (Figures 1 and 2) may allocate the oxidation initiation to oxygen radicals (O). In terms of the oxidation products suggested (viz., propane: propene, acrolein, CO, CO_2, and H_2O; IPr: acetone, CO_2, and H_2O; Ac: CO_2 and H_2O; AcAc: CO_2 and H_2O), the following oxidative dehydrogenation (eqs 1 and

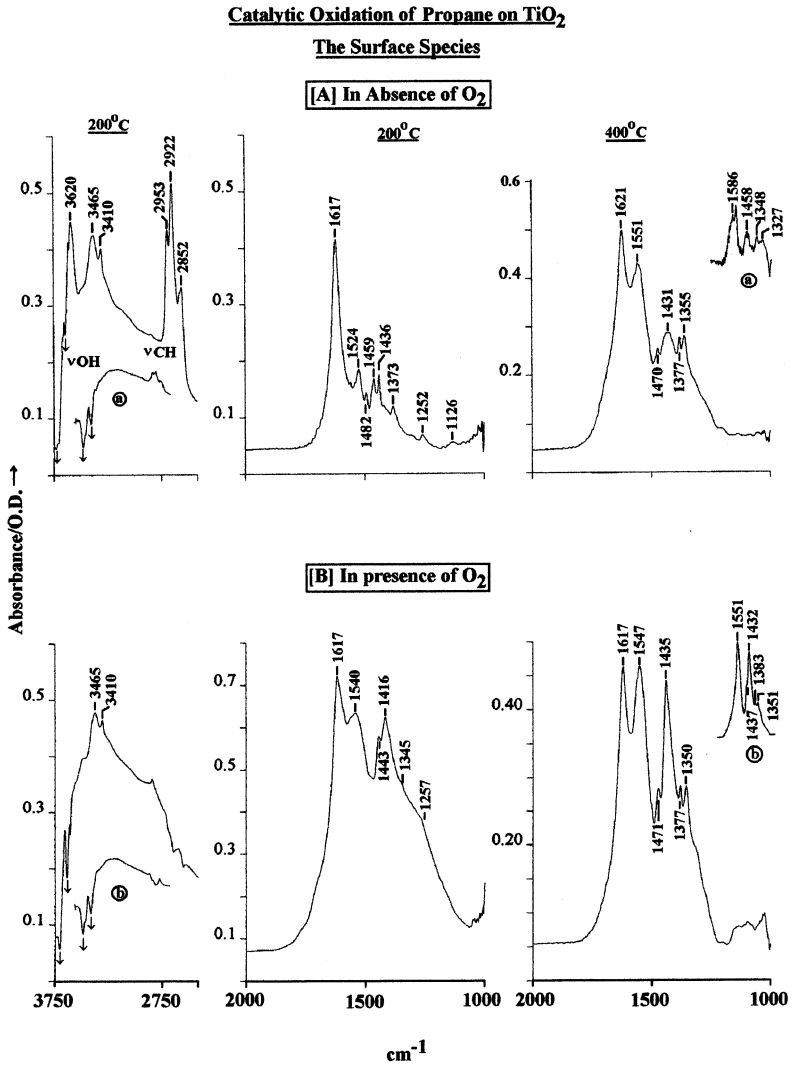

Figure 6. FTIR spectra taken of the adsorbed species of propane on TiO_2 (or ZrO_2; the insets (a) and (b)) established following heating the gas/solid interface at the temperatures indicated (for 10 min), in the absence [A] and presence [B] of oxygen atmosphere (50 Torr).

2) and total oxidation (eqs 3−5) processes may be envisaged:

$$CH_3CH_2CH_3 + O \rightarrow CH_2{=}CHCH_3 + H_2O \quad (1)$$

$$CH_2{=}CHCH_3 + 2O \rightarrow CH_2{=}CH{-}CHO + H_2O \quad (2)$$

$$CH_2{=}CH{-}CHO + 2O + H_2O \rightarrow HCOOH + CH_3COOH \quad (3)$$

$$HCOOH \rightarrow CO + H_2O \quad (4)$$

$$CH_3COOH + 6O \rightarrow 2CO_2 + 2H_2O \quad (5)$$

where O is an oxygen radical.

Although formic and acetic acids are known precursors for formation of carbon oxides and water,[25] the failure to detect them in the reaction mixture might be attributed to their much faster decomposition than formation. Formic acid is thermally less stable than acetic acid, and decomposes directly into CO and H_2O.[25] In contrast, acetic acid requires further oxidation to decompose into CO_2 and H_2O.[25] That a partial oxidation pathway (e.g., eqs 6−8 below) is not suggested, may be ascribed to (i) the marked stability of acetone (Figure 2) would have made it detectable in the gas phase, and (ii) the thermal dehydration step of the 2-propanol (eq 6) is not possible in the wake of the thermal stability of 2-propanol (Figure 2).

$$CH_3CH_2CH_3 + O \rightarrow CH_3CH(OH)CH_3 \rightarrow CH_2{=}CHCH_3 + H_2O \quad (6)$$

$$CH_3CH(OH)CH_3 + O \rightarrow CH_3COCH_3 + H_2O \quad (7)$$

$$2CH_3COCH_3 + 2O \rightarrow 3CH_3COOH + 12O \rightarrow 6CO_2 + 6H_2O \quad (8)$$

Though of limited influence on the overall course of oxidation of propane, the gas-phase oxidation results confirm that the three test oxygenate compounds (IPr, Ac, and AcAc) are much more readily oxidized than propane (Figure 2). They, moreover, reveal that the total oxidation pathway predominates the oxidation course of Ac and AcAc, whereas it is the minor catalytic event in the oxidation course of IPr.

The surface oxidation of propane is shown (Figure 3) to enhance not only the overall conversion of the reactant, but also its total oxidation pathway. Thus, CO_2 and H_2O are the sole detectable oxidation products over the oxide catalysts. The total oxidation activity of the oxide catalysts, as gauged versus a reference Pt/Al_2O_3 catalyst (Figure 3), is shown to increase with the catalyst reducibility; i.e., $ZrO_2 < TiO_2 < CeO_2$.[27,28] Figure

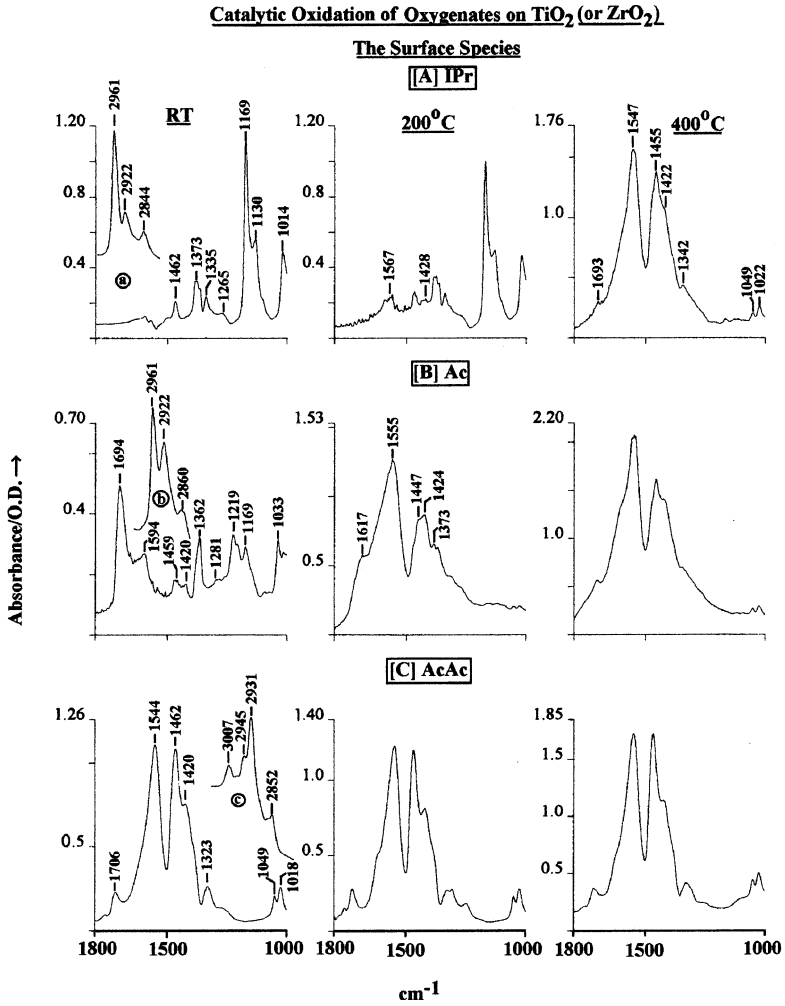

Figure 7. FTIR spectra taken of the adsorbed species of the oxygenate compounds indicated established on TiO_2 (or ZrO_2) following heating the gas/solid interface at the temperatures indicated (for 10 min), in the presence of oxygen atmosphere. The insets (a−c) are the corresponding νCH spectra.

5 may also suggest that the catalyst total oxidation activity may also be promoted by the higher surface acidity of CeO_2. In fact, CeO_2 has been found to expose strong acid and base sites and also acid−base pair sites.[17] The ability of reducible metal sites to interact with hydrocarbon C−H bonds and to cause C−H bond breaking by "oxidative addition" is well-known.[11] These interactions are thought to primarily involve overlapping of d (or f) orbitals of the metal with σ and σ^* orbitals of the C−H bond. CeO_2 is also distinct by a crystal structure (open fluorite structure) quite tolerable to oxygen loss and gain in an almost reversible fashion.[38] It is compatibly considered in some reports[39] a promising solid-state oxygen battery for future fuel cells. Expectedly, the same superior oxidation activity is assumed by CeO_2 toward the oxygenate compounds IPr, Ac, and AcAc (Figure 4). The markedly higher %com, measured in the presence rather than in the absence of oxide catalysts, is evidence for the marked contribution of the surface oxidation. The observed link between the oxidation activity and the catalyst reducibility may assume that the oxidants are lattice oxygen (O^{2-}) rather than adsorbed oxygen ($O_2^{x-}O^{2-}$) species. A Mars-van-Kerelen-type mechanism[28] might, therefore, be considered, particularly that the oxidation activity toward propane, as well as the oxygenate compounds, is triggered at high-temperature regimes ($\geq$300 °C).[40]

Irreversible adsorptive interactions of propane with the oxide surfaces are shown to occur at $\geq$200 °C (Figure 6). They result in formation of two detectable surface species. The initial species is formed at 200 °C (both in the presence and absence of oxygen atmosphere) and remains observed till 400 °C (on TiO_2 but not on ZrO_2). It is characterized by three νCH vibrations (at 2953−2852 cm^{-1}), a sharp, strong IR absorption at 1617 cm^{-1}, and a number of weak δCH and νC−C absorptions at 1436−1126 cm^{-1}. Its formation is accompanied by association (hydrogen-bonding) with surface-OH groups. This species is unlike the adsorbed species observed for IPr, Ac, and AcAc on the oxide surfaces at 200 °C (Figure 7), i.e., it is neither an aldol condensation product of acetone, an isopropoxide, nor an acetate species. It is partially converted into carboxylate (acetate, 1551−1547, 1435−1431, and 1355−1350 cm^{-1}; formate, 1590−1580, 1385−1377, and 1355−1350 cm^{-1})[32] and carbonaceous species (carbonate, 1155−1520 and 1420−1400; bicarbonate, 3340−3150,1610−1600, and 1450−1440 cm^{-1}).[33] The conversion is shown to be enhanced at high temperatures and in the presence of oxygen (Figure 6). The preceding IR characteristics of the surface product of the initial adsorptive interactions of propane may account for a product of oxidative dehydrogenation rather than oxidative addition. In fact, an absorption at 1620−1600 cm^{-1} is either due to νC═C vibration of an olefin that is strongly drained of π-electrons by a strong Lewis acid site, or νC═O of a carbonyl group that is strongly conjugated with a double bond and/or strongly donating electrons to a strong Lewis acid site.[34] Accordingly, the results may suggest the initial adsorbed species of propane/oxide interactions to be either adsorbed propene and/or acrolein. This suggestion may find support by (i) the detection

of propene and acrolein among the products of gas-phase oxidation (Figure 1), and (ii) the possible overlapping of full and empty d-orbitals of surface Lewis acid sites with empty π^* and full π-type orbitals of olefins toward formation of surface π-complexes,[36] and (iii) thus, the instability of this species on ZrO_2 at 400 °C is due possibly to the absence on ZrO_2 of such strong Lewis acid sites. Acetone molecules (localized charge), which assume stronger tendency toward surface interactions than conjugated carbonyl compounds (delocalized charge), have been found[34] to adsorb less strongly on ZrO_2 than on TiO_2 for similar reasons. The following surface reactions are suggested for the formation of the observed surfaces species of propane as a function of temperature:

$$CH_3CH_2CH_{3(g)} + 2M^{4+} + O^{2-} \rightarrow CH_3CH{=}CH_2\cdots M^{4+} + H{-}M^{3+} + HO^- \rightarrow CH_3CH{=}CH_{2(g)} + H_{2(g)} + 2M^{4+} + O^{2-} \quad (9)$$

$$CH_3CH{=}CH_2\cdots M^{4+} + HO^- \rightarrow CH_2{=}CH{-}CH_2O^-\cdots M^{4+} + H_{2(g)} \quad (10)$$

$$CH_2{=}CH{-}CH_2O^-\cdots M^{4+} + M^{4+} \rightarrow CH_2{=}CH{-}CHO\cdots M^{4+} + H{-}M^{3+} \quad (11)$$

$$H{-}M^{3+} + HO^- \rightarrow H_{2(g)} + O^{2-} + M^{4+} \quad (12)$$

$$CH_2{=}CH{-}CHO\cdots M^{4+} + M^{4+} + 2HO^- + O_{2(g)} \rightarrow CH_3CO_2^-\cdots M^{4+} + HCO_2^-\cdots M^{4+} + H_2O_{(g)} \quad (13)$$

$$CO_{2(g)} + O^{2-} + M^{4+} \rightarrow CO_3^{2-}\cdots M^{4+} \quad (14)$$

$$CO_{2(g)} + HO^- + M^{4+} \rightarrow HCO_3^-\cdots M^{4+} \quad (15)$$

It is obvious from eq 9 that the oxidative dehydration active sites are acid−base pair sites with the acid site being a reducible Lewis acid site to facilitate the hydrogen abstraction. Adopting the C−H bond activation model suggested by Finocchio et al.,[11] we suggest the secondary carbon C−H bond to be the target of the initial interaction with the surface by bonding simultaneously to $M^{4+}{-}O^{2-}$ pair sites (the hydrogen to the oxide, and the carbon to the metal site). The formation of acetate and formate surface species necessitates splitting of the $C_2{-}C_1$ bond of the acrolein species. The formation of carbonate/bicarbonate species is facilitated by the presence of CO_2 in the gas phase, which is evident from the spectra shown in Figure 4.

The fact that the present results suggest an oxidative dehydrogenation as the initial catalytic interaction for the total oxidation of propane on the present set of oxides contradicts the results of Finocchio et al.,[25] who have observed enough evidence for an initial oxidative addition of oxygen species in the oxidation course of oxygen-free propane gas phase on calcined $MgCr_2O_4$. These authors[25] have allocated the oxidant function to surface oxygen species bound to Cr(VI), and probably Cr(V), sites arising as a result of a partial surface oxidation during the calcination process applied to the catalyst. Thus, the present results exclude the presence of such excess oxygen species on the test oxide catalysts, a conclusion that can be consolidated by the intolerance of the tetravalent Zr, Ti, and Ce ions to further oxidation.

Conclusions

The above presented and discussed results may facilitate drawing the following conclusions:

(1) Propane is totally oxidized on the test oxides (ZrO_2, TiO_2, and CeO_2) at 300−400 °C to give CO_2 and H_2O into the gas phase.

(2) The oxidation activity of the oxide catalysts ($ZrO_2 < TiO_2 < CeO_2$) is presumably directly related to the oxide reducibility and surface acidity.

(3) The absence of surface excess oxygen species on the test catalysts renders the initial catalytic interaction to involve an oxidative dehydrogenation of propane into propene, rather than an oxidative addition into isopropoxide species.

(4) The subsequent interactions of propene are dominated by an oxidative addition to give acrolein, which suffers an overoxidation and splitting of the $C_1{-}C_2$ bond to result in acetate and formate surface species.

(5) The carboxylate species are the precursors of the eventual total oxidation products (CO_2 and H_2O).

(6) The CO_2 thus produced is involved in surface interactions giving rise to carbonaceous surface species.

(7) The catalytic active sites are suggested to be Lewis acid−base pair sites over which the secondary carbon C−H bond is activated by simultaneous bonding, and the hydrogen abstraction is facilitated by the reducibility of the Lewis acid site.

(8) CeO_2 is a promising material for the chemical makeup of potential oxide catalysts for the total oxidation of hydrocarbons.

Acknowledgment. Kuwait University Research Administration Grant No. SC095 and the excellent technical support found at Analab/SAF of the Faculty of Science are highly appreciated.

References and Notes

(1) Garten, R. L.; Dalla Betta, R. A.; Schlatter, J. C. In *Handbook of Heterogeneous Catalysis*; Ertl, G., Knözinger, H., Weitkamp, J., Eds.; Wiley-VCH: Weinheim, 1997; Vol. 4, pp 1668−1677.

(2) Marchetti, L.; Forni, L. *Appl. Catal. B* **1998**, *15*, 179.

(3) Saracco, G.; Scibilia, G.; Iannibello, A.; Baldi, G. *Appl. Catal. B* **1996**, *8*, 229.

(4) Stojanovic, M.; Mims, C. A.; Houdalla, H.; Yang, Y. L.; Jacobson, A. J. *J. Catal.* **1997**, *166*, 324.

(5) Terlecki-Baricevic, A.; Garbic, B.; Jovanovic, D.; Angelov, S.; Mehandziev, D.; Morinova, C.; Kirilov-Stefanov, P. *Appl. Catal.* **1989**, *47*, 145.

(6) Zwinkels, M.; Jaras, S. G.; Menon, P. G. *Catal. Rev. Sci. Eng.* **1993**, *35*, 261.

(7) Cybulksi, A.; Moulijin, J. *Catal. Rev. Sci. Eng.* **1994**, *36*, 179.

(8) *Chemical Processing Handbook;* McKetta, J. J., Ed.; Dekker: New York, 1993.

(9) Bielanski, A.; Haber, J. *Oxygen in Catalysis*; Dekker: New York, 1991.

(10) Wittcoff, H. A. *ChemTech* **1990**, *20*, 1990.

(11) Finocchio, E.; Busca, G.; Lorenzelli, V.; Willey, R. J. *J. Catal.* **1995**, *151*, 204.

(12) Haber, J. In *Catalysis of Organic Reactions*; Kosak, J. R., Johnson, T. A., Eds.; Dekker: New York, 1994; p 151.

(13) Al-Mashta, F.; Davanzo, C. U.; Sheppard, N. *J. Chem. Soc., Chem. Commun.* **1983**, 1258.

(14) Zaki, M. I.; Hasan, M. A.; Pasupulety, L.; Fouad, N. E.; Knözinger, H. *New J. Chem.* **1999**, *23*, 1197.

(15) Busca, G.; Lorenzelli, V.; Ramis, G.; Sanchez Escribano, V. *Mater. Chem. Phys.* **1991**, *29*, 175.

(16) Busca, G.; Ramis; Lorenzelli, V.; Janin, A.; Lavalley, J. C. *Spectrochem. Acta A.* **1987**, *43*, 489.

(17) Zaki, M. I.; Hasan, M. I.; Al-Sagheer, F. A.; Pasupulety, L. *Colloids Surf.* **2001**, *190*, 261.

(18) Hasan, M. A.; Zaki, M. I.; Pasupulety, L. *J. Mol. Catal. A* **2002**, *178*, 125.

(19) Hussein, G. A. M.; Sheppard, N.; Zaki, M. I.; Fahim, R. B. *J. Chem. Soc., Faraday Trans. 1* **1989**, *85*, 1723.
(20) Mul, G.; Zwijnenburg, A.; Linden, B.; Makkee, M.; Moulijn, J. A. *J. Catal.* **2001**, *201*, 128.
(21) Peri, J. B.; Hannan, R. B. *J. Phys. Chem.* **1960**, *64*, 1526.
(22) Pierson, R. H.; Fletcher, A. N.; Clair Gantz, E. St. *Anal. Chem.* **1956**, *28*, 1218.
(23) *The Aldrich Library of FT-IR Spectra*, 1st ed.; Pouchert, C. J., Ed.; Aldrich Chemical Co.: Milwaukee, WI, 1989; Vol. 3.
(24) Harris, R. K. *Spectrochim. Acta* **1964**, *20*, 1129.
(25) Finocchio, E.; Busca, G.; Lorenzelli, V. *JCS Faraday Trans.* **1994**, *90*, 3347.
(26) Fierro, J. L. G.; Soria, J.; Rojo, J. M. *J. Solid State Chem.* **1987**, *66*, 154.
(27) Haber, J. *J. Less-Common Met.* **1977**, *54*, 243.
(28) Mars, P.; Van Krevelen, D. W. *Chem. Eng. Sci.* **1954**, *3*, 41.
(29) Knözinger, H. In *Surface Organometallic Chemistry: Molecular Approaches to Surface Catalysis*; Basset, J.-M., et al., Eds.; Kluwer Academic Publishers: New York, 1988; pp 35−46.
(30) Tsyganenko, A. A.; Filmonov, V. N. *J. Mol. Struct.* **1973**, *19*, 579.
(31) Zaki, M. I.; Knözinger, H. *Mater. Chem. Phys.* **1987**, *17*, 201.
(32) Bensitel, M.; Moravek, V.; Lamotte, J.; Saur, O.; Lavalley, J.-C. *Spectrochim. Acta* **1987**, *43A*, 1487.
(33) Nakamoto, K. *Infrared Spectra of Inorganic and Coordination Compounds*; J. Wiley: London, 1963; pp 222−224.
(34) Zaki, M. I.; Hasan, M. A.; Pasupulety, L. *Langmuir* **2001**, *17*, 768.
(35) Panov, A.; Fripiat, J. J. *Langmuir* **1998**, *14*, 3788.
(36) Davydov, A. A. *Infrared Spectroscopy of Adsorbed Species on the Surface of Transition Metal Oxides*; Wiley: New York, 1990.
(37) Busca, G.; Lorenzelli, V. *Mater. Chem.* **1982**, *7*, 89.
(38) Ostuka, K.; Hatano, M.; Morikawa, A. *J. Catal.* **1983**, *79*, 493.
(39) Takahashi, T. In *Physics of Electrolytes*; Haldik, J., Ed.; Acdemic Press: London, 1972; Vol. 3, p 989.
(40) Gellings, P. J.; Bouwmeester, H. J. M. *Catal. Today* **1992**, *12*, 1.